Characterizing Implosion Targets using X-ray Thomson Scattering

Andrea Kritcher[1], T. Döppner[1], O.L. Landen[1], S. H.Glenzer[1]
[1]Lawrence Livermore National Laboratory

Abstract

We present the first x-ray Thomson scattering measurements from inertial confinement fusion targets. Spectrally resolved x-ray Thomson scattering has been applied at the Omega Laser Facility to investigate the capsule adiabat of cone-in-shell inertial confinement fusion targets. Here the technique of scattering from implosion targets was developed and tested for use as a diagnostic at the National Ignition Facility (NIF), LLNL. Measurement of the adiabat through measurement of T_e and T_F is applied to test low-adiabat pulse shaping methods, designed for optimum compressibility and stability. Theoretical equation of state models (EOS) can also be tested for implosion conditions, by measuring the temperature, density, and ionization state of the compressed material.

- The non-collective, or microscopic behavior of the plasma, was probed with XRTS of Zn He-alpha x-rays at a scattering angle of 113°.
- For these degenerate plasmas, the width of the inelastic scattering peak is proportional to the Fermi energy, and thus the electron density. The electron temperature is obtained from the measured intensities of the elastic and inelastic features (assuming $T_e = T_i$) due to dependency of the elastic scattering intensity on ion temperature. The calculated adiabat ($(n_e(2.45T_e(T_e/T_F)+(3/5)T_F)+n_iT_i)/(n_e(3/5)T_F)$) is dependent on T_e, T_i, and T_F.
- Theoretical fits to in-flight scattering measurements yield electron densities ranging from 0.06 to $1.1\times10^{24}cm^{-3}$ and temperatures ranging from 6 to 11 eV for varying drive conditions (pulse shaping and drive energy) . The corresponding adiabats ranged from ~10 for the weakly driven, high adiabat implosion, to ~1.2 for a low adiabat, highly compressed implosion.

X-ray Thomson Scattering Theory

X-ray Scattering

$$\alpha = \frac{1}{k\lambda_s} \propto \frac{\lambda}{\lambda_s} \qquad k = \frac{4\pi}{\lambda_o}\sin(\theta/2)$$

We Scatter x-rays from electrons in the plasmas.

Electrons absorb the photon, oscillate, and re-emit the x radiation.

Plasma Screening Length: λ_S

Fermi-degenerate Plasma:

$$\lambda_{TF} = \left(\frac{\hbar^2}{4m_e e^2}\left(\frac{\pi}{3n_e}\right)^{1/3}\right)^{1/2}$$

Classical Plasma:

$$\lambda_D = \left(\frac{\varepsilon_o k T_e}{n_e e^2}\right)^{1/2}$$

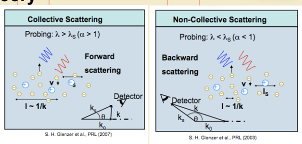

Elastic (Rayleigh):

E of incident photon is conserved

-Tightly Bound e⁻ : Binding Energy > Compton Energy (ΔE_c)

Inelastic (Compton or Plasmon):

E of incident photon is not conserved

-Weakly Bound e⁻ : Binding Energy < Compton Energy (ΔE_c)

-Free e⁻

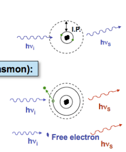

O. L. Landen et al., JQSRT 71, 465 (2001)

Non-Collective Scattering

The frequency of the Compton feature is shifted by:

$$\lambda^* = \lambda_o\left[1 + 2\left(\frac{h\nu}{mc^2}\right)\sin^2\left(\frac{\theta}{2}\right) \pm \left(\frac{v}{c}\right)\sin\left(\frac{\theta}{2}\right)\right]$$

Compton downshifted peak has a distribution proportional to the free electron temperature of the plasma due to Doppler broadening.

For degenerate plasmas, the Compton width is proportional to the Fermi Temperature, thus n_e.

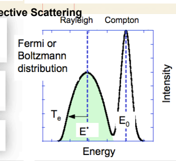

Sensitivity and Future Experiments

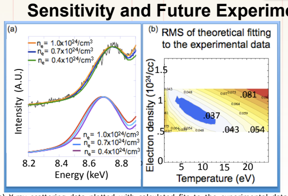

(a) X-ray scattering data plotted with calculated fits to the experimental data including the effect of scattering at multiple k-vectors in previous measurements. Shown on the bottom are calculations of the x-ray scattering spectra for the new design that includes a smaller source size and higher scattering angles, also including the effect of scattering at multiple k-vectors from the capsule. Here, the electron density is varied to show sensitivity of the Compton width to electron density, while the ionization state is 2.3 and Te=Ti= 6 eV. (b) RMS values of theoretical fitting to the experimental data showing sensitivity in determining the electron density and temperature (Te=Ti) to experimental data. Here, Be(+2.3).

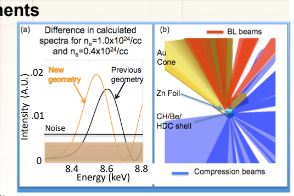

(a) Difference as a function of energy between simulated scattering spectra that were calculated for different electron densities. Here, the difference is a result of the change in the Compton width for increasing ne. (orange) Is the difference for the new geometry (black) Is for the old geometry. Also shown are the noise levels. (b) The new experimental configuration where a Zn BL foil for the probe generation is placed on the side of the Au cone to result in higher scatter angles and a smaller range of k-vectors, for higher sensitivity of the Compton feature to electron density.

Experimental Setup

Zinc He-α x-rays, produced from intense laser irradiation (~1.7·10¹⁵Wcm⁻²) of 10 μm thick Zn foils, were scattered from the compressed CH shell. The CH shell was compressed using intense lasers (each ~3·10¹³ Wcm⁻² with SG4 800 μm phase plates) in a semi-spherical geometry. X-rays were scattered from the compressed CH at an angle of 113° and recorded using a HOPG Bragg spectrometer (ZSPEC).

Omega Chamber

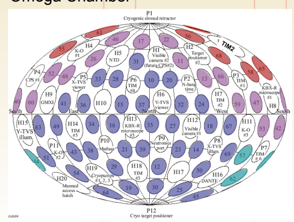

- Drive Beams
- Back Lighter Beams
- Beams that clipped the gold cone
- Beams that interfered with the ZSPEC and Ni shield

Diagnostics:
- -ZSPEC in Tim6 to record the scattered spectra
- -SSCA in Tim2 to look at the Zn He-alpha BL source
- -Pinhole cameras in Tim4 and Tim5 to look at the implosion (Fixed)
- -Henway- Look at source spectrum
- -Dante- to view the CH shell x-ray flux
- -Integrated Pinhole: Implosion and BL

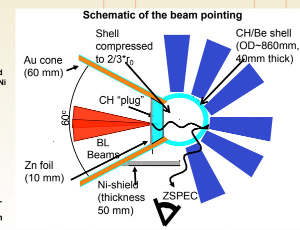

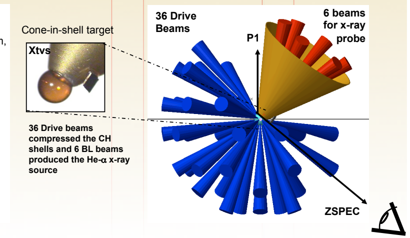

36 Drive beams compressed the CH shells and 6 BL beams produced the He-α x-ray source

Simulations

Radiation hydro-dynamic simulations of the mass density of imploding CH and Be shells as a function of radius and time since the start of the compression. Also plotted are the laser intensity profiles (white) as a function of time (axis on the top of the plot).

Radiation Hydrodynamic modeling using the 1D code HELIOS.* The 1D simulations provide a basis for experimental planning, but cannot take into account the complex 3D geometry of the cone-in-shell targets. Future calculations with LASNEX** would be extremely beneficial.

CH Shell: LA370901p

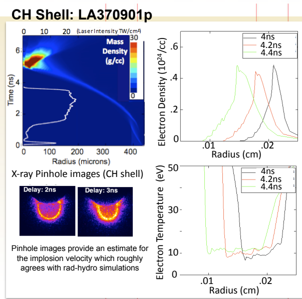

Pinhole images provide an estimate for the implosion velocity which roughly agrees with rad-hydro simulations

Be Shell: LA370901p

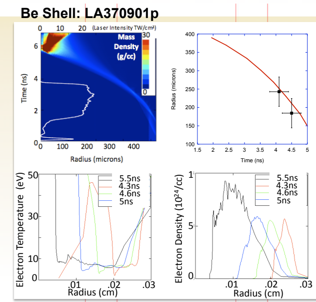

Be Shell: LA2201

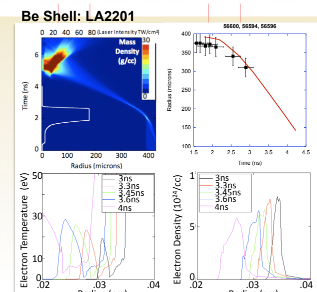

Experimental Measurements

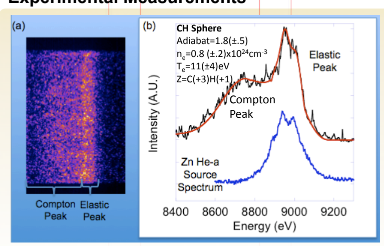

In-Flight (4.2 ns after the start of the drive beams) x-ray scattering data ((a) raw and profiles (b)) from laser compressed CH cone-in-shell targets (see CH Shell: LA370901p for the drive pulse shape). Theoretical fits to the experimental data yields temperatures, densities, and ionization states of about $0.8\times10^{24}cm^{-3}$, 11 eV, and C(+3)H(+1). Also plotted is the Zn He-α probe source spectrum (blue).

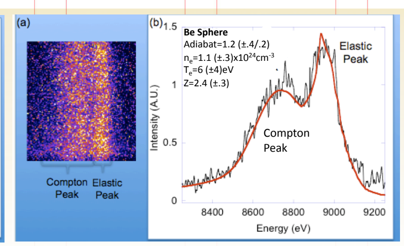

In-Flight (3.1 ns after the start of the drive beams) x-ray scattering data ((a) raw and profiles (b)) from laser compressed Be cone-in-shell targets (see CH Shell: LA370901p for the drive pulse shape). , including an elastic feature and a Compton down-scattered peak. Theoretical fits to the experimental data yields temperatures, densities, and ionization states of about $1.1\times10^{24}cm^{-3}$, 6 eV, and Be(+2.3).

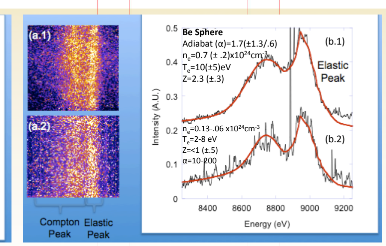

Data shown in a.1 and b.1 characterize a full energy drive configuration (385J/beam, LA2201 at 3.06 ns) and data in a.2 and b.2 result from scattering from a weakly driven implosion (150J/beam, LA2201 at 4.66 ns). Theoretical fits to the experimental data yield temperatures, densities, and ionization states of about $0.7\times10^{24}cm^{-3}$, 10 eV, and Be(+2.3) for b.1. For b.2, the data suggested strong temperature and density gradients and were fit with a convolution of theoretical spectra at ($0.13\times10^{24}cm^{-3}$ and 2.2 eV) and ($0.06\times10^{24}cm^{-3}$ and 8 eV), both with Z<1.

Lawrence Livermore National Laboratory

National Ignition Facility • Lawrence Livermore National Laboratory • Operated by the US Department of Energy
This work performed under the auspices of the U.S. Department of Energy by Lawrence Livermore National Laboratory under Contract DE-AC52-07NA27344.

NIF National Ignition Facility